J. Fluid Mech. (1965), *vol.* 21, *part* 1, *pp.* 97–106
Printed in Great Britain

Puff motions in unstratified surroundings

By J. M. RICHARDS
Department of Electrical Engineering, Loughborough College of Technology

(Received 24 March 1964 and in revised form 18 August 1964)

The fluid motion associated with puffs (strongly turbulent masses of fluid moving through surroundings with which they mix readily) is considered, for cases in which any buoyancy force acts in the direction of gross motion, the surroundings are unstratified, the internal and external densities are approximately equal, and the motion of the surroundings is directly associated with the motion of the puff. It is assumed that the size of any one such puff is directly proportional to the distance travelled, i.e. that $r = z/n$.

It is shown that $d\{\rho r^a (dz/dt)\}/dt = C_a M_a g$, where t is time, ρ is the density of the surrounding fluid, g is the gravitational acceleration, C_a is a numerical constant, and $a = 3$ or 2 in the cases of axial or planar mean symmetry. M_3 is the mass excess, and M_2 is the mass excess per unit length.

Previous experiments with buoyant puffs having zero initial momentum (i.e. experiments with thermals) confirm these equations and give the values $C_2 \simeq 0{\cdot}33$ and $C_3 = 0{\cdot}27$. New experiments with non-buoyant puffs having considerable initial momentum also confirm the equations, with the same values for C_2 and C_3. These results support the view that the turbulence inside thermals is primarily maintained through their mean motion rather than directly by gravitational instability.

1. Introduction

A thermal is a strongly turbulent mass of buoyant fluid moving, due only to the action of buoyancy forces, through surrounding fluid with which it can mix freely. Early experiments with isolated thermals of constant total buoyancy in unstratified surroundings (Scorer 1957; Woodward 1959) showed that each thermal roughly obeyed the equation

$$z = nr, \tag{1}$$

where z is the distance travelled by the leading extremity of the turbulent region, $2r$ is the greatest horizontal dimension of the turbulent region, and n is a number which was constant for any one thermal; the value of n varied considerably from thermal to thermal. The mean fluid motion was roughly symmetrical about a vertical axis: such cases are therefore called axial thermals.

Later experiments (Richards 1963) showed that, in circumstances like those of Scorer's and Woodward's experiments, cylindrical thermals (i.e. thermals in which the mean motion is roughly symmetrical about a vertical plane) obey (1). In cylindrical thermals, $2r$ is the maximum dimension perpendicular to the

vertical plane of mean symmetry. These and other experiments (Richards 1961) also showed that, during the motion of any one thermal,

$$z^{a+1} = {}_xC_a^2 n^a M_a g t^2/\rho, \tag{2}$$

where ρ is the density of the surrounding fluid, t is the elapsed time, g is the acceleration due to gravity, ${}_xC_a$ is a numerical constant for all thermals of the one type, and $a = 3$ or 2 for axial or cylindrical thermals respectively. M_3 is the constant mass excess of an axial thermal (the difference between the masses of fluid contained within and displaced by the thermal) and M_2 is the mass excess per unit length of a cylindrical thermal. The experimental results gave ${}_xC_3 = 0{\cdot}73$, and ${}_xC_2 \doteq 0{\cdot}7$ when the thermal was released almost instantaneously.

In other experiments (Turner 1962) increasing values of M_3 were imitated by the progressive generation and growth of small gas bubbles within a liquid thermal which moved through unstratified surroundings. One is therefore led to consider the more general case of a strongly turbulent buoyant or non-buoyant element which moves through and mixes with its surroundings. Such an element is called a puff. Axial puffs of zero initial buoyancy were studied experimentally by Grigg & Stewart (1963); the present work extends and clarifies their results.

2. Special cases of puff motion

The general case of puff motion is so complicated, for example by the possible stratification of potential density and velocity in the surroundings, that we first consider puff motions with the following restrictions:

(i) any buoyancy force acts only in the direction of motion of the puff as a whole;

(ii) the internal and external densities are approximately equal, but this approximation does not apply to the calculation of buoyancy forces;

(iii) the motion of the surrounding fluid is substantially only associated with the motion of the puff itself;

(iv) the surrounding fluid is unstratified.

The experiments with thermals then lead us to suppose that the distributions of velocity in any single puff may be similar at all stages of the motion, so that (1) is obeyed by any one puff. The same experiments show that n may vary considerably from puff to puff, and we must therefore consider what approximate similarity may exist between puffs having differing values of n. Consider any two isolated puffs which have, at a certain instant, equal values of r but very different values of n. Observations show that each puff maintains a roughly spherical or cylindrical shape, and so, at that instant, r is approximately a linear measure of the size of either turbulent region. Since the size of the turbulent region is a feature of the distribution of velocity, and since the values of z are very different at the chosen instant, the length scale of the velocity distribution must be independent of z if this distribution is roughly similar in any two puffs. For the same reasons, it is appropriate to assume that r is a length scale of the velocity distribution. The proper choice of a velocity scale is more difficult; it will be assumed that the velocity distribution has a velocity scale dz/dt, that is a velocity

scale roughly equal to the velocity of advance of the most turbulent fluid. These assumptions are apparently supported by the results which follow.

By symmetry, the impulse of an axial puff is directed along the line of action of the buoyancy force. By restriction (ii) above, this impulse is directly proportional to the product of a characteristic velocity with the density of the fluid and the cube of a characteristic linear dimension of the puff. The impulse of any axial puff is therefore roughly directly proportional to $\rho r^3(dz/dt)$. Similarly, the impulse per unit length of a cylindrical puff is roughly directly proportional to $\rho r^2(dz/dt)$. In either case, the factor of proportionality should not vary much from puff to puff.

The rate of change of the impulse is equal to the buoyancy force; the momentum equations for axial and for cylindrical puffs, under the foregoing restrictions, therefore become

$$\left.\begin{aligned} d\{\rho r^3(dz/dt)\}/dt &= C_3 M_3 g \quad \text{for axial puffs,} \\ d\{\rho r^2(dz/dt)\}/dt &= C_2 M_2 g \quad \text{for cylindrical puffs,} \end{aligned}\right\} \tag{3}$$

where C_3 and C_2 are numerical factors which vary little from puff to puff.

We next consider the results of experiments on thermals and their relation to (3).

3. Thermals of constant buoyancy

When a thermal moves through unstratified surroundings after release with zero initial momentum, and when M_3 or M_2 is constant, equations (3) give

$$\rho r^3(dz/dt) = C_3 M_3 g t, \quad \rho r^2(dz/dt) = C_2 M_2 g t. \tag{4}$$

If we substitute for r in these equations, from (1), and again integrate with respect to time, we find

$$z^4 = n^3 2 C_3 M_3 g t^2/\rho, \quad z^3 = n^2 3 C_2 M_2 g t^2/2\rho. \tag{5}$$

Equations (5) explain the occurrence of the terms n^3 and n^2 in (2); these terms were originally obtained empirically. Comparing (2) with (5), we obtain

$$2C_3 = {}_xC_3^2, \quad 3C_2 = 2{}_xC_2^2. \tag{6}$$

The experimental values ${}_xC_3 = 0{\cdot}73$, ${}_xC_2 \simeq 0{\cdot}7$ (Richards 1961, 1963) may be substituted in (6) to give corresponding values for C_2 and C_3; these values are

$$C_3 = 0{\cdot}27, \quad C_2 \simeq 0{\cdot}33. \tag{7}$$

4. Puffs of zero buoyancy; experiments

In the case of an axial or a cylindrical puff which is everywhere equal in density to its surroundings, we have M_3 or $M_2 = 0$. If restrictions (iii) and (iv) of § 2 still apply, (3) may be integrated twice, using (1), to give

$$z^4 = 4C_3 n^3 I_3 t/\rho, \quad z^3 = 3n^2 C_2 I_2 t/\rho, \tag{8}$$

where I_3 is the initial momentum of an axial puff and I_2 is the initial momentum per unit length of a cylindrical puff.

Such non-buoyant puffs have been produced experimentally in a rectangular water tank. Figure 1 (*a*) represents the central vertical cross-section of the puff-producing apparatus. This 'puffer' extended horizontally between transparent parallel vertical walls of the experimental tank when cylindrical puffs were to be produced, but the puffer was much shorter when axial puffs were required. The puffers were closed on all sides, and the tops too could be closed by stoppers A (see figures 1 (*b*) and (*c*)). A plane wire gauze mat was fixed horizontally across the inside of each puffer. In the cylindrical puffer this mat was placed at about the level of the free surface of the water in the tank, but in the axial puffer the mat was at the orifice.

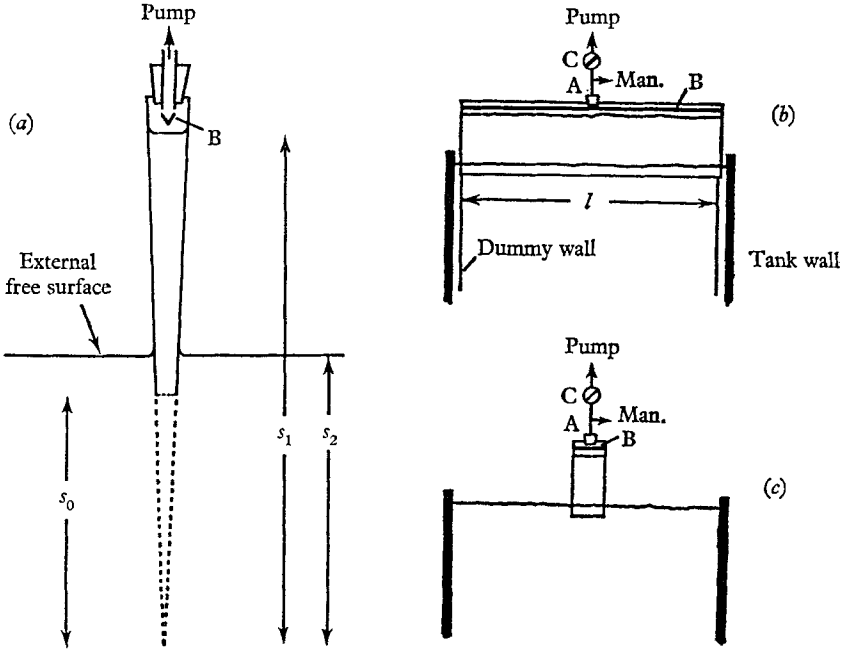

FIGURE 1. The apparatus, or 'puffers', which were used to produce dyed non-buoyant puffs. (*a*) Cross-section of puffer. B is a small fixed trough which held dyed water. (*b*) Schematic side elevation of the puffer which was used to produce cylindrical puffs. The cross-section is shown in (*a*). The dummy-walls—large square sheets of thin glass—made the mean motion two-dimensional. (*c*) Schematic side elevation of the puffer which was used to produce axial puffs. Cross-section shown in (*a*).

In order to produce a puff, the stopper was inserted and the air pressure inside the puffer was gradually reduced until the trough B, which held a small volume of dyed water, was swamped. The internal air pressure was then increased gradually until the water surface inside the puffer reached a convenient level, and then the tap C was closed. When dye from the trough had mixed, by slow convection, throughout the water contained in the puffer, the stopper A was suddenly withdrawn. This action released the mass of dyed water, which fell quickly out of the puffer under its own weight. Considerable turbulence was generated within the mass by its sudden passage through the gauze mat, and so a dyed puff was formed near the top of the experimental tank.

The shape of the axial puffer may cause surprise. A puffer in the form of a vertical cylindrical tube was tried at first, but this design was abandoned when preliminary experiments showed that the tube often produced a turbulent vortex ring rather than a puff.

The puff motions were recorded by ciné photography; the ciné camera also recorded the indications of a clock (which registered to 0·01 sec) and of a water manometer. This manometer, which was connected to 'Man.' in figure 1 (*b*) and (*c*), was used to register the difference between the levels of the free surfaces inside and outside the puffer immediately before the removal of the stopper A.

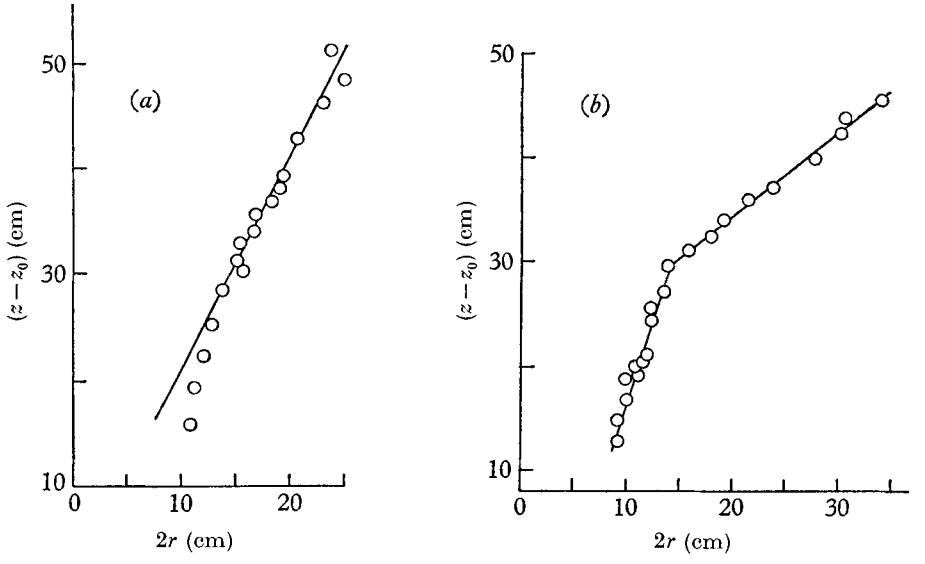

FIGURE 2. (*a*) The relationship between the distance, z, travelled by the cap of a typical non-buoyant puff, and the greatest width of the puff, $2r$. The graph represents an axial puff, but the corresponding graphs for cylindrical puffs were very like this. (*b*) An unusual variation of z with r, which was observed only once, in an axial puff.

Observations from above showed that puffs from the axial puffer only became roughly axisymmetric after the distance travelled became roughly equal to the length of the longer sides of the puffer orifice. The experimental record of the earliest part of each such experiment was therefore ignored. Corresponding values of the distance $(z-z_0)$ of the front of each puff from the puffer orifice, of $2r$, and of the time $(t-t_0)$ from an arbitrary origin, were measured by projection from the ciné film. A graph of $(z-z_0)$ against $2r$ was then plotted for each experiment, and the slope $\frac{1}{2}n$ and intercept z_0 were found. A typical example of such a·graph is shown in figure 2 (*a*). In all but one of the experiments, as in the experiment which corresponds to figure 2 (*a*), n was roughly constant throughout the observed motion. In the exceptional case, which was an axial puff, the value of n suddenly changed during the course of the experiment—the relevant graph of $(z-z_0)$ against $2r$ is reproduced in figure 2 (*b*). This sharp change is all the more interesting because no like change has yet been observed in any experiments with thermals. The reason for the change is unknown; the fact that the values of

n which occurred in the two parts of the exceptional experiment were also the greatest and least values which were observed in any axial puff perhaps indicates that the stability of the distribution of fluid velocity associated with a puff motion is less at the higher values of n.

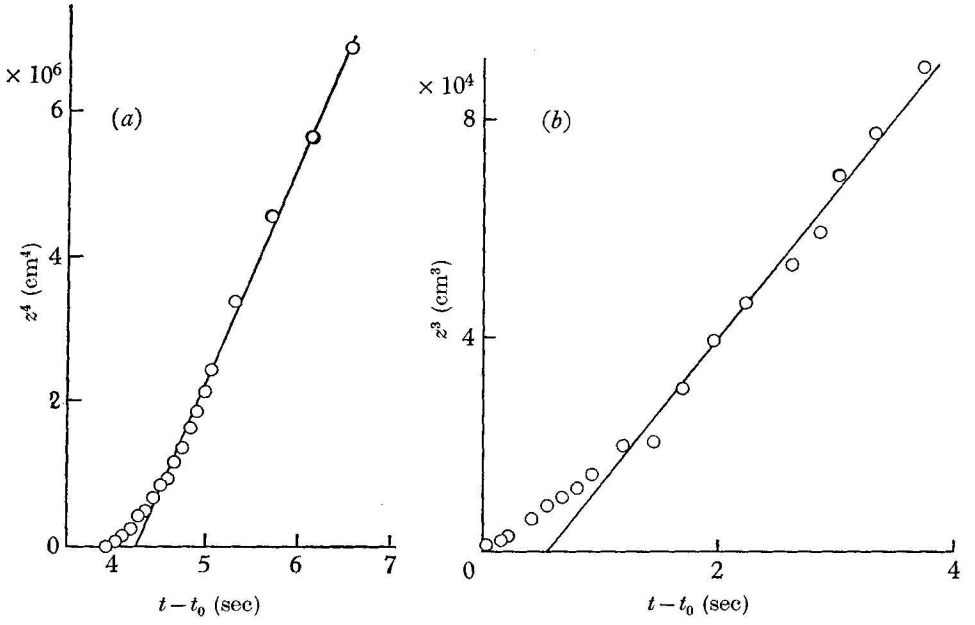

FIGURE 3. The relationship between distance travelled, z, and time, in typical cases: (a) non-buoyant axial puff; (b) non-buoyant cylindrical puff.

The intercept of each graph like figure 2(a) with the axis $2r = 0$ gave the corresponding value of z_0, and from this was calculated the value of z corresponding to each value of $2r$. In the case of figure 2(b), the two parts of the graph were treated separately as if they belonged to separate experiments, and so then two values of z_0 were obtained. In order to verify (8), a graph of z^4 against $(t-t_0)$ was plotted for each normal axial puff, and for each part of the exceptional puff, and a graph of z^3 against $(t-t_0)$ was plotted for each cylindrical puff. Typical cases are shown in figure 3. In the exceptional case, the graph of z^4 against $(t-t_0)$ was sharply divided into an earlier and a later part, and could be correspondingly represented by two distinct straight lines. The transition between the two parts was apparently simultaneous with the corresponding change in the value of n already noted.

From (8)

$$\frac{dz^4}{dt}\Big/\frac{I_3}{\rho} = 4C_3n^3, \quad \frac{dz^3}{dt}\Big/\frac{I_2}{\rho} = 3C_2n^2, \tag{9a,b}$$

for axial and cylindrical puffs, respectively. Corresponding values of n and dz^4/dt or dz^3/dt could be found from the slopes of the two graphs for each experiment, and C_3 and C_2 are known from the results of § 3. So that (9) could be tested experimentally, it was therefore only necessary to estimate I_3/ρ or I_2/ρ for each puff.

5. Estimates of I_3/ρ and I_2/ρ

The longer sides of each puffer were made of transparent rigid plastic sheets. In subsidiary experiments, the air pressure inside each puffer was adjusted, as before, so as to obtain some convenient difference of level between the internal and external water surfaces, and the motions of these surfaces were then photographed in an interval of time which included and immediately followed the removal of the stopper. The clock was again included in the field of view of the ciné camera.

An examination of individual frames of these ciné films revealed that the free surface of the water inside each puffer remained roughly plane and horizontal during its descent. Also, the amplitudes of the waves created on the water surface outside the puffer were very much less than any of the initial differences of level used in the main experiments. This result was obtained intentionally, by fixing the puffer orifice at a constant and sufficient depth (about 4 cm) below the initial level of the external free surface. After its first descent, the internal free surface heaved slightly about the final level, but remained roughly horizontal. The ratio of successive maximum displacements above the final level during these small oscillations was roughly 0·9.

Consider a horizontal plane situated at a short distance below the puffer orifice. Let dI_3^x/dt be the downward flux of momentum through this plane. Then

$$dI_3^x/dt = \int \rho u |u| \, dA,$$

where u is the downward vertical component of the fluid velocity, and dA is the element of area. It will be assumed that we may approximate to this integral by $-A|\dot{V}|\dot{V}\rho/A^2$, where $\dot{V}$ is the rate of change of the volume of water within the puffer, and A is the area of the puffer orifice. This assumption is equivalent in effect to an assumption that the velocity component is uniform across the region of area A and zero elsewhere.

Let s be the distance of the free surface inside the puffer above the line in which the internal planes of the sides would meet if produced (figure 1(*a*)). Let s_0 be the distance of the puffer mouth above this line, and let s_1 and s_2 be, respectively, the initial and final values of s. Let I_3^x be the momentum emitted by the puffer. Then from the assumption of the preceding paragraph, it follows easily that

$$I_3^x \simeq \frac{\rho A}{4s_0^2} \int_{s_1^2}^{s_2^2} \frac{d(s^2)}{dt} \, d(s^2). \tag{10}$$

Since the amplitude of the oscillations of the internal free surface was always much less than the initial head of water, and since these oscillations were only slightly damped, the total efflux of momentum immediately following the first coincidence of the internal free surface with its final level was presumably almost equal to the subsequent influx until the second coincidence, and so on during the successive quarter cycles of oscillation. The small remainder of the momentum flux may reasonably be supposed to have been converted to momentum of small-scale eddies and of waves on the external free surface. The value of I_3^x

corresponding to the motion of the internal free surface from its initial level to its first coincidence with its final level is therefore an approximate estimate of the total impulse of the puff, that is, of I_3 or of I_2/l in the cases of axial and of cylindrical puffs respectively, where l is the length of the mouth of the puffer which was used to produce cylindrical puffs.

The ciné film record of each subsidiary experiment was projected and measured frame by frame so as to determine corresponding values of t and s, and a graph of s^2 against t was plotted for the interval between the removal of the

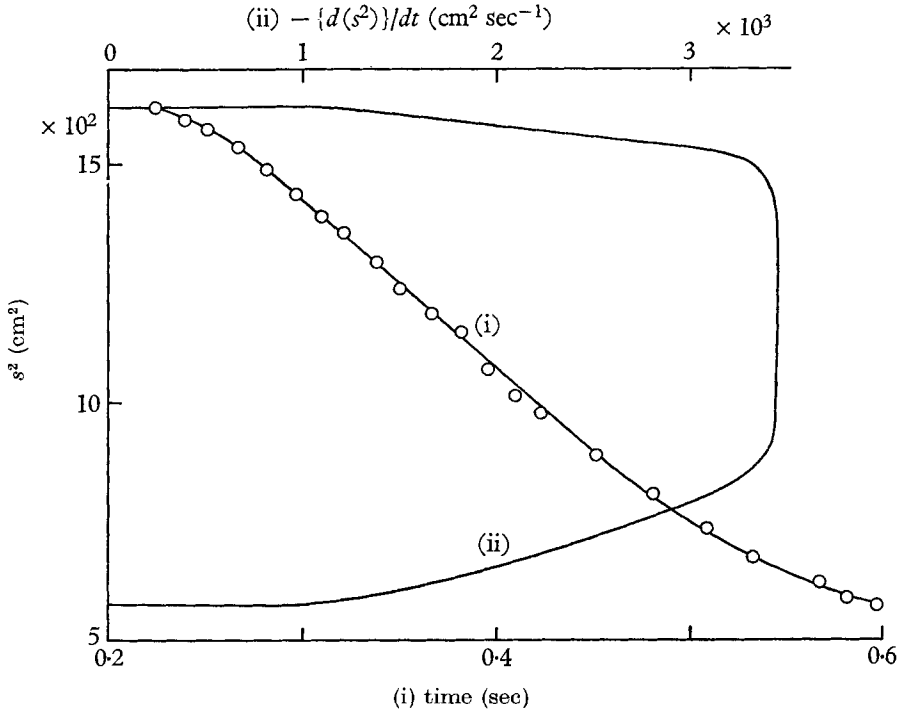

FIGURE 4. A subsidiary experiment for estimating the impulse of a non-buoyant puff. The area between curve (ii) and the axis of s^2 is approximately proportional to the impulse; see equation (10).

stopper and the first coincidence of the free surfaces. The slope of each graph was estimated at various points by drawing tangents, and so corresponding graphs of $-ds^2/dt$ against s^2 were constructed. The area under each graph, equal to the integral in (10), was measured with a planimeter. The values of A, s_0, and l were measured, and so I_3/ρ or I_2/ρ was estimated. An example of the graphs of s^2 against t and of $-ds^2/dt$ against s^2 is shown in figure 4. In each set of subsidiary experiments, the value of s_2 was fixed at the value which had been used in the main experiments, and the range of initial head $(s_1 - s_2)$ included the corresponding range in the main experiments. Graphs of I_3/ρ and I_2/ρ against $(s_1 - s_2)$ were then plotted, and these graphs were used to convert the value of $(s_1 - s_2)$ recorded by the water manometer in each main experiment into a corresponding estimate of I_3/ρ or I_2/ρ.

6. Results

The value of $(dz^4/dt)/(I_3/\rho)$ in each experiment on an axial puff was estimated as the quotient of the slope of the corresponding graph like figure 3(*a*) and the corresponding estimate of I_3/ρ; the value of n for each experiment was measured from the slope of the corresponding graph like figure 2(*a*). These results are shown in figure 5(*a*), in which the full line represents (9*a*) with the value of C_3 given by (7). Similarly, figure 5(*b*) shows the corresponding values of $(dz^3/dt)/(I_2/\rho)$ and of n for the cylindrical puffs. Here, the full line represents (9*b*) with the value of C_2 given by (7). Thus a useful degree of agreement has

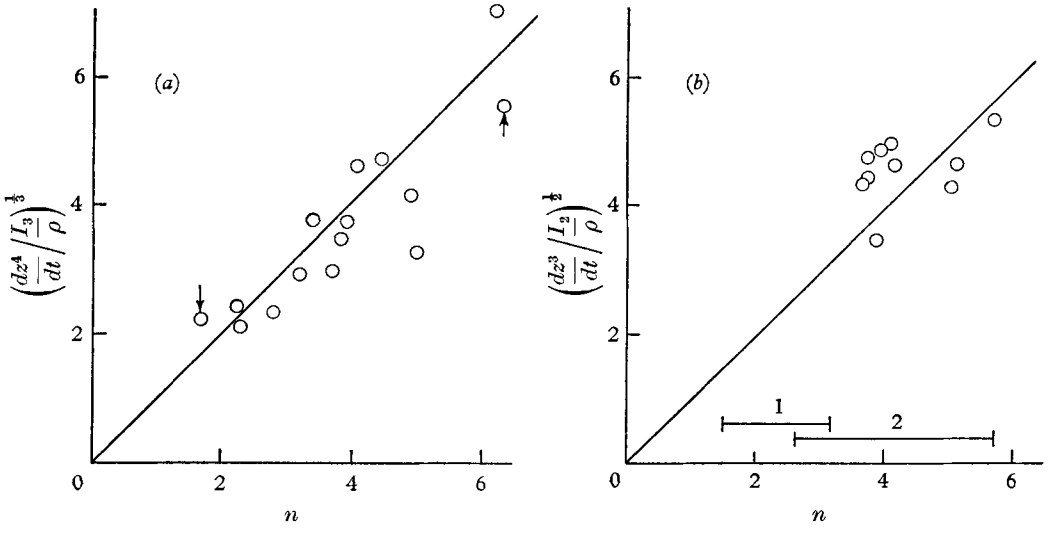

FIGURE 5. The encircled points are pairs of values from observations on non-buoyant puffs. The straight lines represent equations (9) with the values of C_2 and C_3 found from earlier experiments on thermals (Richards 1961, 1963). The lines fit the observations quite well; this shows that non-buoyant puffs and thermals have roughly the same values of C_2 and C_3. (*a*) Axial case. Arrowed points represent the two parts of the unusual puff of figure 2(*b*). (*b*) Cylindrical case. 1, Range of n observed in thermals. 2, Range of n observed in puffs. Unfortunately, an experimental mishap prevented the measurement of I_2 for the experiments which had the lowest values of n.

been established between these experiments and the predictions of § 4. When n changed suddenly in the course of a particular experiment, the separate parts of the experiment separately confirmed the predictions (figure 5(*a*)).

The mean distribution of fluid velocity inside and outside a cylindrical non-buoyant puff was found by the method previously used for cylindrical thermals (Richards 1963). If the result, figure 6, is compared with typical corresponding results for thermals (Richards 1963) it is clear that these distributions are very alike. The initial turbulence in a thermal is generated by static instability during the earliest part of the motion. In contrast, the initial turbulence in these puff experiments was generated by shear in the wake of a wire mesh. However, the mean velocity distributions in the final stages of the two motions are alike, and we have seen that the experiments give equal values for C_2 and C_3. Static instability, which was absent in the puff experiments, therefore seems to be

excluded as the main mechanism by which turbulence is maintained in thermals. We may presumably conclude that the turbulence of both buoyant and non-buoyant puffs is primarily maintained by the mean motion. If there is buoyancy, the buoyancy primarily maintains only the mean motion.

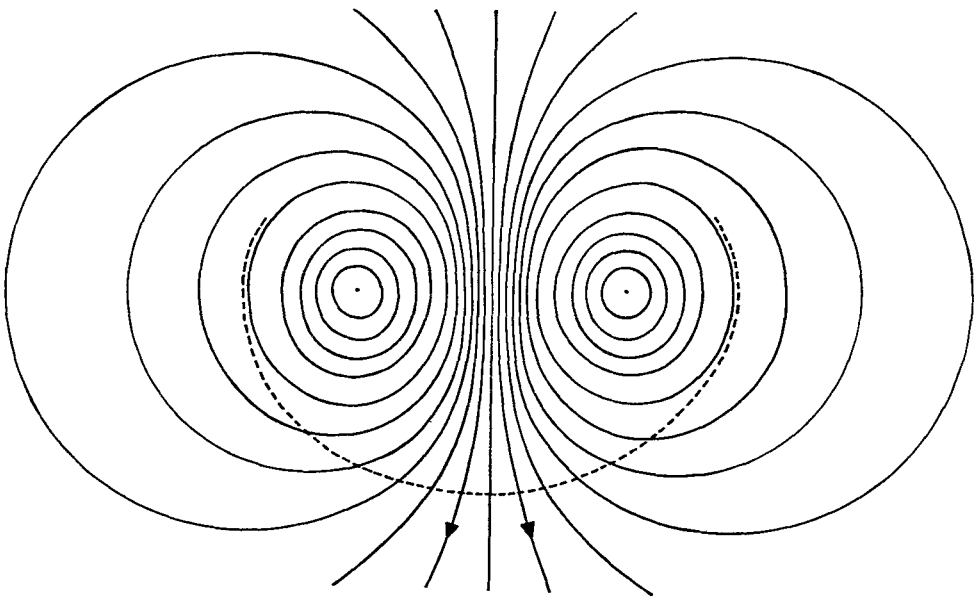

FIGURE 6. The mean fluid motion associated with a non-buoyant cylindrical puff. The full lines represent streamlines of a mean normalized stream function ψ^*, which is defined from the ordinary stream function ψ by $\psi^* = \psi/(z(dz/dt))$. The lines are drawn at equal intervals of ψ^*, and the increment of ψ^* between adjacent lines is 0·02. The line – – – – marks part of the boundary of the puff. The puff was moving as though towards the bottom of this page, and the value of n was 3·4. Arrows indicate the direction of fluid motion. The flow outside the puff approximates closely to the potential flow due to a line doublet of strength $0{\cdot}034z^2(dz/dt)$ per unit length. The mean fluid motion associated with this puff is very like the mean motion associated with cylindrical thermals (Richards 1963).

The restriction of § 3 to cases of zero initial momentum is easily removed. For example, in unstratified surroundings, if $M_3 g$ and $M_2 g$ are constant, (5) must be replaced by

$$z^4 = 2C_3 n^3 (M_3 gt + 2I_3)\, t/\rho, \quad z^3 = 3C_2 n^2 (M_2 gt + 2I_2)\, t/2\rho, \tag{11}$$

for axial and cylindrical puffs respectively. In the earliest part of such motions the initial impulse is dominant, and (11) approximate to (8). Later, when the impulse due to buoyancy becomes dominant, (11) approximate to (4).

I wish to thank Mr J. Rippon, who helped to construct and operate the apparatus.

REFERENCES

GRIGG, H. R. & STEWART, R. W. 1963 *J. Fluid Mech.* **15**, 174.
RICHARDS, J. M. 1961 *J. Fluid Mech.* **11**, 369.
RICHARDS, J. M. 1963 *Int. J. Air Wat. Poll.* **7**, 17.
SCORER, R. S. 1957 *J. Fluid Mech.* **2**, 583.
TURNER, J. S. 1962 *Quart. J. Roy. Met. Soc.* **89**, 62.
WOODWARD, B. 1959 *Quart. J. Roy. Met. Soc.* **85**, 144.